Organic Electronics 11 (2010) 1719–1722

Contents lists available at ScienceDirect

Organic Electronics

journal homepage: www.elsevier.com/locate/orgel

Atomic layer deposited HfO_2 gate dielectrics for low-voltage operating, high-performance poly-(3-hexythiophene) organic thin-film transistors

Woo-Jun Yoon [a], Paul R. Berger [a,b,*]

[a] Department of Electrical and Computer Engineering, The Ohio State University, Columbus, OH 43210, USA
[b] Department of Physics, The Ohio State University, Columbus, OH 43210, USA

ARTICLE INFO

Article history:
Received 11 April 2010
Received in revised form 23 July 2010
Accepted 26 July 2010
Available online 6 August 2010

Keywords:
High-*k* gate dielectric
Atomic layer deposition
Organic thin-film transistor
Field-effect mobility
Poly-(3-hexythiophene)

ABSTRACT

Here we report on low-supply voltage and high-performance regioregular poly-(3-hexythiophene) (P3HT) organic thin-film transistors (OTFT) using a thin atomic layer deposited (ALD) HfO_2 gate dielectric. For the capacitance–voltage characteristics, the measured gate capacitance was ~392 nF/cm^2 at 1 kHz and the dielectric constant was estimated ~18.5 for a 40 nm thick ALD HfO_2 gate dielectric. The gate dielectric showed breakdown fields >5 MV/cm with the leakage current density less than 10^{-7} A/cm^2 at 2 MV/cm. With octadecyltrichlorosilane-treated ALD HfO_2 gate dielectrics, P3HT OTFTs demonstrated high field-effect mobilities up to ~0.01 ± 0.002 cm^2/V s in the saturation region with the drain voltage of −5 V, which is at least one order of magnitude higher than typically reported mobilities particularly for low-voltage regioregular P3HT OTFTs using high-*k* inorganic gate dielectrics. The threshold voltage in the saturation region and on–off current ratio were measured to be −1.2 ± 0.2 V and ~1.1(±0.1) × 10^4, respectively.

1. Introduction

The performance of organic thin-film transistors (OTFT) have, in general, made tremendous progress in the last decade [1–3]. Using sublimed low molecular weight organic and solution-processed polymeric materials, excellent OTFT results have been reported paving the way for niche applications, such as radio-frequency technologies [4], and pixel drivers and switching elements for active-matrix displays [5,6].

Among the various conjugated polymers for the active channel layer in OTFTs, regioregular poly-(3-hexythiophene) (P3HT) has been one of the most popular channel materials in organic electronics due to its simple solution processibility and relatively high device performance. Stemming from its lamellar structure [7], P3HT films have reported relatively high carrier mobility (μ) in the range of ~0.1 cm^2/V s to ~0.3 cm^2/V s [8–11]. However, extremely high operating voltages persisting up to 60 V are often required to obtain saturation in OTFTs with low-dielectric constant (k) materials for the gate dielectric layer. Alternatively a variety of high-*k* gate dielectrics using inorganic, polymeric, and self-assembled monolayer or multilayer gate dielectrics, has been successfully implemented in OTFTs, greatly reducing OTFTs operating voltages and exhibiting excellent device performance [12,13].

For P3HT OTFTs particularly with metal oxide high-*k* dielectrics, high OTFT performance with low-supply operating voltages have been reported, as summarized in the Table 1 [14–17]. While hafnium-based oxide gate dielectrics were frequently employed in pentacene OTFTs [18,19], it has not yet been reported for regioregular P3HT OTFTs. In this article, we report low-voltage operation (sub −5 V) and high-performance P3HT OTFTs with an atomic layer deposited (ALD) HfO_2 gate dielectric.

* Corresponding author at: Department of Electrical and Computer Engineering, The Ohio State University, Columbus, OH 43210, USA. Tel.: +1 614 247 6235; fax: +1 614 292 7596.
E-mail address: pberger@ieee.org (P.R. Berger).

1566-1199/$ - see front matter © 2010 Elsevier B.V. All rights reserved.
doi:10.1016/j.orgel.2010.07.026

Table 1
Summary of the performance of P3HT OTFTs using metal oxide high-k gate dielectrics; thickness (t_{ox}), accumulation capacitance of metal oxide gate dielectric (C_{ox}), drain voltage (V_D), dielectric constant (k), saturation mobility (μ_{sat}), and threshold voltage (V_T); e-beam – electron-beam evaporation, ALD – atomic layer deposition.

Refs.	Dielectric material	Deposition method	t_{ox} (nm)	C_{ox} (nF/cm^2)	V_D (V)	k	μ_{sat} (cm^2/V s)	I_{on}/I_{off}	V_T (V)
[14]	Ta_2O_5	e-Beam	100	89	0 to −3.0	20.2	2.0×10^{-2}	2.0×10^3	+0.26
[15]	Al_2O_3	ALD	50	–	–	–	4.1×10^{-4}	7.0×10^4	−3.6
[15]	Al_2O_3[a]	ALD	50	–	–	–	9.2×10^{-3}	∼54	+5.6
[16]	Al_2O_3[a]	Anodization	6	625	0 to −2.5	4.2	5.0×10^{-3}	n/a	−1.2
[17]	TiO_2	Sputtering	51	750	0 to −5.0	43.2	1.5×10^{-2}	1.0×10^3	−1.0
This work	HfO_2[a]	ALD	40	392	0 to −5.0	18.6	1.1×10^{-2}	1.2×10^4	−1.4

[a] A self-assembled monolayer of octadecyltrichlorosilane (OTS) treatment applied to the oxide surface.

2. Experimental

The HfO_2 films were deposited on silicon substrates with a commercial ALD reactor. During deposition, the ALD chamber temperature was set at 250 °C. All silicon substrates used in this study were processed through standard degreasing and RCA cleaning procedures prior to the deposition. The thicknesses (t) and the refractive index of the deposited films were estimated to be ∼40 nm and ∼2.07, respectively, as measured by single wavelength ellipsometry.

For capacitance–voltage (C–V) characteristics with an LCR meter (Agilent 4284A), the HfO_2 was deposited on p-type silicon wafers with a resistivity of ∼4.4 Ω cm for metal–oxide-semiconductor (MOS) capacitors. All HfO_2 gate dielectrics were used without any annealing. After deposition, MOS capacitors were completed by standard photolithography and lift-off of the Au (100 nm) gate, defining a square area of 80 μm by 80 μm. A Ti adhesive layer with a 15 nm thickness is used to increase the adhesion between the Au electrode and the ALD films. The final MOS structure fabricated was a p-Si/HfO_2/Ti/Au. The leakage current density through the MOS capacitors was measured with a semiconductor parameter analyzer (Agilent 4156) at room temperature and in darkness.

For the bottom contacted OTFTs, a heavily doped n-type silicon substrate with a resistivity of ∼0.003 Ω cm was used as the gate. The source and drain contacts are formed by standard photolithography and lift-off of the Au (100 nm) with a 15 nm Ti adhesive layer, defining a channel length of 7 μm and width of 115 μm atop the ALD HfO_2 layer. It should be noted that a Ti adhesion layer could affect the charge carrier transport between the source and the drain, requiring an optimized thickness [23]. In this work, the thickness of a Ti adhesive layer was not optimized. After photolithography and metal lift-off, the surface of the HfO_2 was plasma cleaned using an inductively coupled plasma reactive ion etching system with oxygen at an RF power of 20 W for 1 min. To modify the gate dielectric surface, a self-assembled monolayer (SAM) of octadecyltrichlorosilane (OTS; Aldrich, assay >90%) was then formed by immersing the ALD HfO_2 films in a 25 g/L solution of OTS dissolved in cyclohexane at ∼5 °C for 20 min, as described by Majewski et al. [20]. Thin films of the P3HT were then deposited by spin coating from a concentration of 8 mg/ml in chloroform in an inert glove box environment with ⩽1 ppm level of oxygen and moisture. The regioregular P3HT (Merck Chemicals, Ltd.) with 94.5% regioregularity was used without further purification. The P3HT used here has a weight-average molecular weight (M_w) of 26,200 g/mol, corresponding to a number-average molecular weight (M_n) of 13,000 g/mol, and with a polydispersity (M_w/M_n) of ∼2. The P3HT OTFTs were kept in a vacuum at pressures below 10^{-6} Torr for 10 h to remove any unintended doping. Prior to the measurement, the completed P3HT OTFTs were briefly annealed at 110 °C for 10 min in N_2 atmosphere. Small trenches in the P3HT film around the source and drain electrodes were created with a needle in order to minimize leakage currents [20]. Electrical characterizations of the P3HT OTFTs were performed with a semiconductor parameter analyzer (Agilent 4156) at room temperature under darkness in ambient air.

3. Results and discussion

In addition to the OTFTs, MOS capacitors were also studied as a control. Fig. 1 shows a typical C–V response of the ALD HfO_2 MOS capacitors at a frequency range from 1 kHz to 1 MHz at room temperature under darkness. The varying frequency response clearly shows accumulation at negative

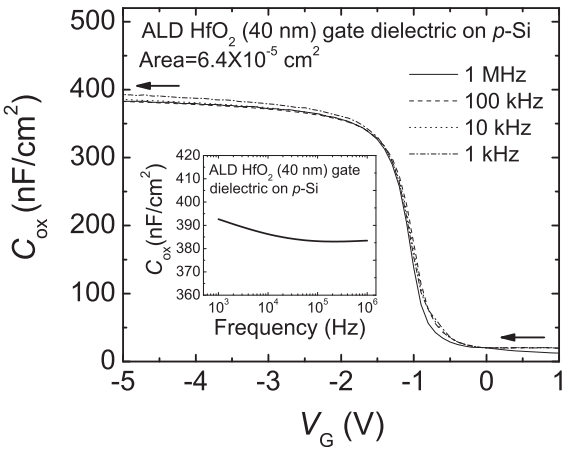

Fig. 1. Capacitance–voltage (C–V) characteristics of MOS capacitors at various frequencies for an atomic layer deposited HfO_2 (∼40 nm) gate dielectric (p-Si/HfO_2/Ti/Au). The inset shows frequency dependency of the gate capacitance per area (C_{ox}) in accumulation and the dielectric constant. The extracted k value at 1 kHz is ∼18.5.

gate bias voltages and depletion at positive gate bias voltages. The hysteresis behavior of the capacitor was observed, exhibiting ~0.5 V hysteresis at 1 MHz (not shown here). The trap charge density (N_t) in the gate dielectric layer is estimated to be $\sim 1.1 \times 10^{11}$ cm^{-2} using the relation $N_t = C_{ox} \cdot \Delta/q$, where C_{ox} is the measured gate capacitance per unit area (F/cm^2), Δ is a voltage shift (V), and q is the magnitude of electronic charge (C). The C_{ox} tends to shift to slightly higher values when decreasing the frequency for all capacitors, as shown in the inset of Fig. 1. No postdeposition heat treatment was used to densify, or passivate, the HfO_2 prior to OTFT fabrication. An observed frequency dependent dispersion in the accumulation region can be attributed to the slow polarization of the gate dielectric at higher frequencies and this polarization can lead to an increase in the induced charge at lower frequencies. The dielectric constant (k) of the ALD HfO_2 gate dielectric was calculated at four different frequencies using $k = C_{ox} \cdot t/\varepsilon_0$, where ε_0 is the permittivity in vacuum, and t is the thickness. The calculated dielectric constants varied from 18.1 at 1 MHz to 18.5 at 1 kHz. For the extraction of carrier mobility values of P3HT OTFTs, the C_{ox} equal to 392 nF/cm^2 at 1 kHz was considered. Upon the addition of the OTS SAM (k = ~2.4 and t = ~2.8 nm) [16], the total capacitance (C_{total}) is considered to be ~262 nF/cm^2 using $1/C_{total} = 1/C_{ox} + 1/C_{OTS}$.

Fig. 2 illustrates the leakage current density versus electric field for the ALD HfO_2 gate dielectric studied here. The dielectric layer shows breakdown fields >5 MV/cm with a leakage current density less than 10^{-7} A/cm^2 at 2 MV/cm for a ~40 nm thick film. The inset of Fig. 2 is the leakage current density versus the gate voltage characteristics for the MIS capacitors.

Fig. 3a shows the output characteristics for P3HT OTFTs with an applied drain voltage (V_D) ranging from 0 to −5 V with a gate bias (V_G) varying from 1 to −5 V in steps of −1 V. The output curves are typical for p-type OTFTs operating in an accumulation region. The OTFTs function well at low-supply voltages due to the high gate capacitance of HfO_2. The inset of the Fig. 3a is a photomicrograph of the Au source–drain contacts atop the ALD HfO_2 gate dielectric.

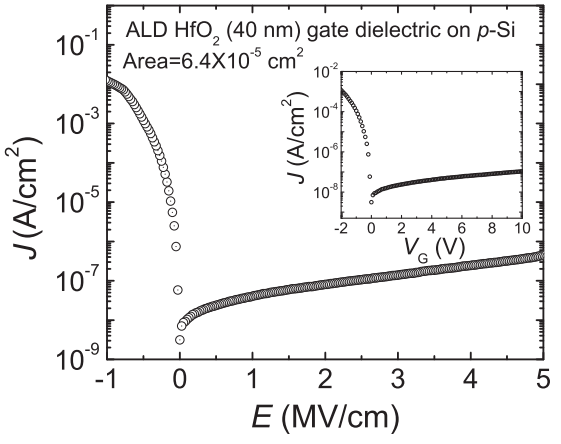

Fig. 2. The leakage current density (J) as a function of electric field (E) of MOS capacitors (p-Si/HfO_2/Ti/Au). The breakdown field is estimated >5 MV/cm. The inset shows current density–voltage characteristics of the devices.

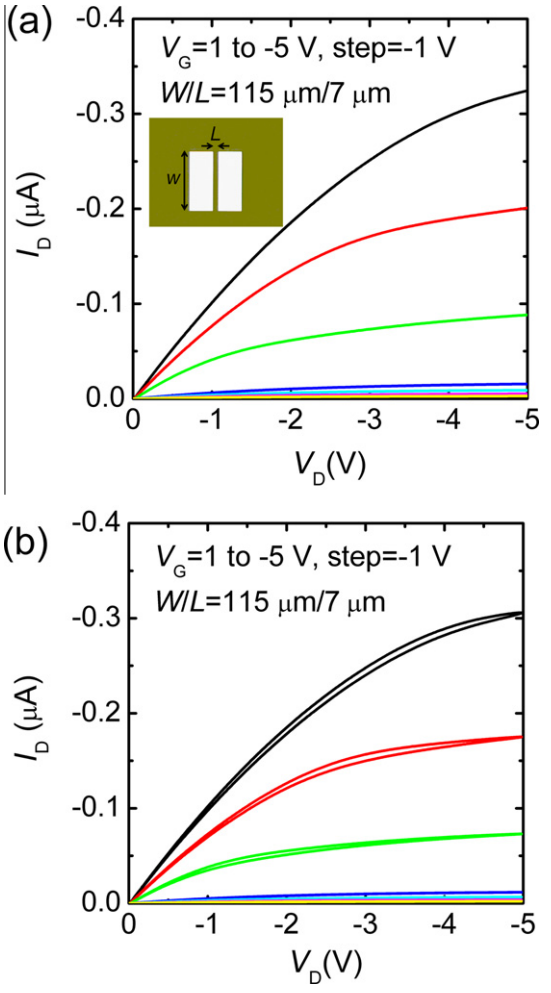

Fig. 3. (a) The output characteristics for P3HT OTFTs with the applied drain voltage (V_D) ranging from 0 to −5 V with gate biases (V_G) varying from 0 to −5 V in steps of −1 V. The inset is the image of the Au source–drain contacts atop the ALD HfO_2 gate dielectric using standard photolithography and lift-off process. (b) The hysteresis behavior of the output characteristic of P3HT OTFTs for an applied voltage V_D (0 → −5 V → 0 V).

At V_G = −2 V and V_D = 0 V, a very small positive I_D of $\sim 2.5 \times 10^{-11}$ A is observed, which increased with higher V_G due to a small drain-gate leakage current. For an applied voltage V_D (0 → −5 V → 0 V), a small hysteresis was observed at V_G > −3 V, and no significant hysteresis behavior was shown for gate voltages less than −3 V (Fig. 3b).

During the electrical measurements in ambient air, a variation of off-state I_D at V_G = 0 V and V_D = −5 V was carefully monitored. For fresh devices, a small off-state I_D (>$\sim 1 \times 10^{-11}$ A) was observed. However, an off-state I_D (>$\sim 1 \times 10^{-9}$ A) was increased by two orders of magnitude over the extended exposure (about 60 min) in ambient air due to the high bulk conductivity of P3HT attributed from unreduced P3HT and oxygen doping [21,22]. The devices exhibiting a high off-state I_D (>$\sim 1 \times 10^{-9}$ A) typically show significant hysteresis behavior at V_G > −3 V due to large excess drain current. Those devices are excluded from extraction of the performance of the OTFTs in this work.

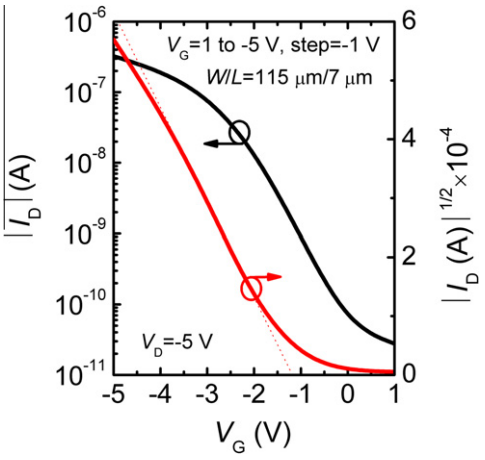

Fig. 4. The saturation region transfer characteristic for P3HT OTFTs with ALD HfO_2 gate dielectrics (~40 nm) with the applied gate voltage (V_G) ranging from 1 V to −5 V with the drain voltage (V_D) of −5 V.

For the transfer characteristics in the saturation region, the saturation mobility (μ_{sat}), the threshold voltage (V_T), and an on/off current ratio (I_{on}/I_{off}) are characterized. Fig. 4 shows the semilog plot of I_D–V_G and the square root of I_D–V_G at $V_D = -5$ V. The μ_{sat}, and the V_T are calculated from

$$I_D = \frac{W}{2L} C_{total} \mu (V_G - V_r)^2 \quad (1)$$

From the square root of I_D as a function of V_G, the maximum μ_{sat} was estimated to be $\sim 0.01 \pm 0.002$ cm^2/V s and the V_T was -1.2 ± 0.2 V. No significant variation of estimated μ_{sat} and V_T was recorded over more than 10 devices. The mobility obtained in this work is one to two orders of magnitude higher than the reported mobilities in low-voltage operating regioregular P3HT OTFTs specifically with metal oxide high-k gate dielectrics, such as ALD Al_2O_3 [15] and anodized Al_2O_3, but was the same order of magnitude mobility using electron-beam evaporated Ta_2O_5 [14], and TiO_2 [17]. Table 1 shows a summary of these gate dielectrics exclusively employed for P3HT OTFTs and their corresponding device performances. For the semilog plot of I_D–V_G at a fixed $V_D = -5$ V, an I_{on}/I_{off} as large as $\sim 1.1(\pm 0.1) \times 10^4$ was measured here, which is similar with previous values reported for P3HT OTFTs using high-k dielectric gate dielectrics (Table 1). From the subthreshold regime in the plot of log I_D as a function of V_G, the subthreshold swing (S) was calculated using $S = dV_G/d(\log I_D)$ and yielded a value of 0.803 ± 0.243 V/decade.

4. Conclusions

In conclusion, we have shown low-voltage operation and high-performance regioregular P3HT OTFTs using ALD HfO_2 gate dielectrics. For the C–V characteristics, the measured C_{ox} was ~392 nF/cm^2 at 1 kHz and the dielectric constant was estimated to be ~18.5 for a 40 nm thick ALD HfO_2 gate dielectric. The HfO_2 gate dielectric showed a breakdown field >5 MV/cm with a leakage current density less than 10^{-7} A/cm^2 at 2 MV/cm. With OTS-treated ALD HfO_2 gate dielectrics, P3HT OTFTs show high mobility up to $\sim 0.01 \pm 0.002$ cm^2/V s in the saturation region, which is at least one order of magnitude higher than typically reported mobilities for low-voltage operating regioregular P3HT OTFTs particularly with metal oxide high-k gate dielectrics. The V_T and I_{on}/I_{off} ratio are -1.2 ± 0.2 V and $\sim 1.1(\pm 0.1) \times 10^4$, respectively.

Acknowledgements

The authors would like to thank Dr. Jill S. Becker and Ray Ritter at Cambridge NanoTech (Cambridge, MA) for ALD deposition. This work was supported by the Center for Photovoltaics Innovation and Commercialization (PVIC) and the Institute for Materials Research (IMR).

References

[1] C.D. Dimitrakopoulos, P.R.L. Malenfant, Adv. Mater. 14 (2002) 99–117.
[2] H.E. Katz, Chem. Mater. 16 (2004) 4748–4756.
[3] H. Sirringhaus, Adv. Mater. 17 (2005) 2411–2425.
[4] V. Subramanian, P.C. Chang, J.B. Lee, S.E. Molesa, S.K. Volkman, IEEE Trans. Compon. Pack. T 28 (2005) 742–747.
[5] H.E.A. Huitema, G.H. Gelinck, J.B.P.H. van der Putten, K.E. Kuijk, C.M. Hart, E. Cantatore, D.M. de Leeuw, Adv. Mater. 14 (2002) 1201–1204.
[6] M. Kitamura, T. Imada, Y. Arakawa, Jpn. J. Appl. Phys. 42 (2003) 2483.
[7] D.M. Richard, Adv. Mater. 10 (1998) 93–116.
[8] B.H. Hamadani, D. Natelson, Appl. Phys. Lett. 84 (2004) 443–445.
[9] J. Park, S. Lee, H.H. Lee, Org. Electron. 7 (2006) 256–260.
[10] C. Shinuk, L. Kwanghee, Y. Jonathan, W. Guangming, M. Daniel, J.H. Alan, S. Mathieu, L. Roberto, J. Appl. Phys. 100 (2006) 114503.
[11] M. Surin, L. Ph, R. Lazzaroni, J.D. Yuen, G. Wang, D. Moses, A.J. Heeger, S. Cho, K. Lee, J. Appl. Phys. 100 (2006) 033712.
[12] A. Facchetti, M.H. Yoon, T.J. Marks, Adv. Mater. 17 (2005) 1705–1725.
[13] J. Veres, S. Ogier, G. Lloyd, D.M. de Leeuw, Chem. Mater. 16 (2004) 4543–4555.
[14] C. Bartic, H. Jansen, A. Campitelli, S. Borghs, Org. Electron. 3 (2002) 65–72.
[15] L. Fumagalli, D. Natali, M. Sampietro, E. Peron, F. Perissinotti, G. Tallarida, S. Ferrari, Org. Electron. 9 (2008) 198–208.
[16] L.A. Majewski, R. Schroeder, M. Grell, P.A. Glarvey, M.L. Turner, J. Appl. Phys. 96 (2004) 5781–5787.
[17] G. Wang, D. Moses, A.J. Heeger, H.-M. Zhang, M. Narasimhan, R.E. Demaray, J. Appl. Phys. 95 (2004) 316–322.
[18] S.W. Cho, J.G. Jeong, S.H. Park, M.H. Cho, K. Jeong, C.N. Whang, Y. Yi, Appl. Phys. Lett. 92 (2008) 213302.
[19] J. Tardy, M. Erouel, A.L. Deman, A. Gagnaire, V. Teodorescu, M.G. Blanchin, B. Canut, A. Barau, M. Zaharescu, Microelectron. Reliab. 47 (2007) 372–377.
[20] L.A. Majewski, R. Schroeder, M. Voigt, M. Grell, J. Phys. D Appl. Phys. (2004) 3367.
[21] M.S.A. Abdou, F.P. Orfino, Y. Son, S. Holdcroft, J. Am. Chem. Soc. 119 (1997) 4518–4524.
[22] D.B.A. Rep, A.F. Morpurgo, T.M. Klapwijk, Org. Electron. 4 (2003) 201–207.
[23] A. Petrovic, G. Bratina, Eur. Phys. J. B 73 (2010) 341–346.